

PQCD Calculation for $\Lambda_b \rightarrow \Lambda\gamma$ in the Standard Model

Xiao-Gang He^{1,2}, Tong Li¹, Xue-Qian Li¹, and Yu-Ming Wang¹

¹Department of Physics, Nankai University, Tianjin

²NCTS/TPE, Department of Physics, National Taiwan University, Taipei

Abstract:

We calculate the branching ratio of $\Lambda_b \rightarrow \Lambda\gamma$ in the standard model using the PQCD method. The predicted branching ratio $B(\Lambda_b \rightarrow \Lambda\gamma)$ can be as large as 1×10^{-7} , with reasonable parameter ranges in the heavy baryon distribution amplitude. This branching ratio is much smaller than those obtained in other hadronic model calculations. Future experimental data can provide important information on the PQCD method for heavy baryon radiative decay and also information about possible new physics beyond the standard model.

PACS numbers: 13.30.Ce, 12.38.Bx, 14.20.Mr

I. INTRODUCTION

Rare radiative processes involving $b \rightarrow s\gamma$ at quark level are important in understanding the flavor changing structure in the standard model (SM). Exclusive radiative B decays also provide important information about the hadronic matrix elements where a heavy b-quark is involved. These processes being rare can also provide important information about models beyond the SM. There have been considerable studies on inclusive $b \rightarrow s\gamma$ [1, 2], and exclusive mesonic $B \rightarrow K^*\gamma$ [3] both experimentally and theoretically within and beyond the SM [4, 5]. Theoretical predictions for inclusive decays agree with data very well in the SM. Calculations for exclusive processes are in general consistent with data although there are unavoidable uncertainties due to our lack of good understanding of QCD at low energies. Nevertheless methods have been developed to calculate hadronic matrix elements in recent years [6, 7]. With more data becoming available, new b decay processes can be studied. These processes can provide new tests for different methods in calculating hadronic matrix elements and new physics beyond the SM. In this work we study $\Lambda_b \rightarrow \Lambda\gamma$. In this decay more experimental information about the heavy b quark inside the hadron which is not available in inclusive and mesonic b-hadron decays, such as spin polarization during hadronization, and the handedness of the couplings at the quark level, can be extracted[8, 9, 10, 11, 12]. Therefore the baryonic b-hadron radiative decay not only can provide a new test for theoretical methods for b-quark hadronization, but also can provide information about new physics beyond the standard model.

There are some studies in the literature on $\Lambda_b \rightarrow \Lambda\gamma$ [8, 9, 10, 11, 12] decay ranging from phenomenological models to QCD sum rule approaches. Our study will be based on the PQCD method[13, 14, 15]. This method has been shown to provide consistent results for two body mesonic B decays[7]. We expect a PQCD calculation for $\Lambda_b \rightarrow \Lambda\gamma$ will also give a reasonable estimate since the energy exchanged by gluons in the matrix element calculations is large. Result obtained in this way can serve as a good reference for discussing the relevant hadronic matrix elements and also new physics beyond the SM.

In the SM the effective Hamiltonian for $b \rightarrow s\gamma$ comes from the electromagnetic penguin diagram and is given by[16]:

$$H_{eff} = i \frac{G_F}{2\sqrt{2}} V_{tb} V_{ts}^* \frac{e}{4\pi^2} C_7^{eff}(\mu) m_b \bar{s} \sigma_{\mu\nu} (1 + \gamma_5) b F^{\mu\nu}, \quad (1)$$

where $C_7^{eff}(\mu = m_b) = -0.31$. In our numerical calculations, the running of C_7^{eff} will also be taken into account.

It has been shown that there may be resonant (long distance) $J/\psi(\psi')$ contributions[17]. If these contributions are included, one should add a term $(3C_1(\mu) + C_2(\mu))(3/\alpha_{em}^2) \sum_{j=\psi, \psi'} \omega_j(0) k_j \pi \Gamma(j \rightarrow l^+ l^-) M_j / (q^2 - M_j^2 + i M_j \Gamma_j^{tot})$ to the Wilson coefficient C_7^{eff} . Since for $b \rightarrow s\gamma$ process, $q^2 = 0$, there are double suppressions for the long distance resonant contributions with one of them coming from the Breit-Wigner factor $\sim \Gamma_i/M_i$ and another coming from the extrapolation of $\omega_j(M_i^2) = 1$ to $\omega_j(0)$ with $\omega_j(0) < 0.13$ (and could be smaller)[17], we will neglect the resonant contribution for radiative decays in our later discussions.

At the hadron level, the decay amplitude for $\Lambda_b \rightarrow \Lambda\gamma$ is obtained by inserting the effective Hamiltonian between the initial and final hadron states,

$$M(\Lambda_b \rightarrow \Lambda\gamma) = \langle \Lambda\gamma | H_{eff} | \Lambda_b \rangle. \quad (2)$$

There are two form factors for $\Lambda_b \rightarrow \Lambda\gamma$ from the above which we write as

$$M_\mu \equiv \langle \Lambda(p') | C_7^{eff}(\mu, 0) \bar{s} \sigma_{\mu\nu} q^\nu (1 + \gamma_5) b | \Lambda_b(p) \rangle = \overline{\Lambda(p')} (F_L \sigma_{\mu\nu} q^\nu (1 - \gamma_5) + F_R \sigma_{\mu\nu} q^\nu (1 + \gamma_5)) \Lambda_b(p). \quad (3)$$

We obtain

$$\Gamma(\Lambda_b \rightarrow \Lambda\gamma) = \frac{G_F^2 |V_{tb}|^2 |V_{ts}|^2 \alpha_{em}^2 |C_7^{eff}|^2 m_b^2}{32 m_{\Lambda_b}^3 \pi^4} (m_{\Lambda_b}^2 - m_\Lambda^2)^3 (|F_L|^2 + |F_R|^2). \quad (4)$$

Emission of a photon from the tree operators $O_{1,2}$ can also contribute to $\Lambda_b \rightarrow \Lambda\gamma$. Although the Wilson coefficients of these operators are larger than those of the penguin operators, there is a large suppression coming from the CKM factor $|V_{ub} V_{us}^* / V_{tb} V_{ts}^*|$. The overall contributions from bremsstrahlung of a photon off the operator $O_{1,2}$ is therefore suppressed. We will neglect their contribution in the rest of the discussions.

II. PQCD CALCULATION OF THE HADRONIC MATRIX ELEMENTS

We now describe the calculations for the hadronic matrix elements defined above using the PQCD method developed in Ref.[13, 14, 15]. We define, in the rest frame of Λ_b , p , p' to be the Λ_b , Λ momenta, k_i ($i = 1, 2, 3$) to be the valence

quark momenta inside Λ_b , and k'_i to be the valence quark momenta inside Λ . We parameterize the light cone momenta with all light quark and baryon masses neglected as

$$\begin{aligned} p &= (p^+, p^-, \mathbf{0}_T) = \frac{M_{\Lambda_b}}{\sqrt{2}}(1, 1, \mathbf{0}_T), \quad p' = (p'^+, 0, \mathbf{0}_T) \\ k_1 &= (p^+, x_1 p^-, \mathbf{k}_{1T}), \quad k_2 = (0, x_2 p^-, \mathbf{k}_{2T}), \quad k_3 = (0, x_3 p^-, \mathbf{k}_{3T}) \\ k'_1 &= (x'_1 p'^+, 0, \mathbf{k}'_{1T}), \quad k'_2 = (x'_2 p'^+, 0, \mathbf{k}'_{2T}), \quad k'_3 = (x'_3 p'^+, 0, \mathbf{k}'_{3T}) \end{aligned} \quad (5)$$

where x_i and x'_i are the fractions of the longitudinal momenta of the valence quarks with $x_1 + x_2 + x_3 = 1$ and $x'_1 + x'_2 + x'_3 = 1$. \mathbf{k}_{iT} and \mathbf{k}'_{iT} are the transverse momenta of the valence quarks inside Λ_b and Λ , respectively.

One can write $p'^+ = \rho p^+$ with $\rho = \frac{2p \cdot p'}{M_{\Lambda_b}^2} = \frac{p'^2 + p'^2 - q^2}{M_{\Lambda_b}^2}$. The ranges for q^2 and ρ are given by $0 \leq q^2 \leq (M_{\Lambda_b} - m_\Lambda)^2$ and $2m_\Lambda/M_{\Lambda_b} \leq \rho \leq (M_{\Lambda_b}^2 + m_\Lambda^2)/M_{\Lambda_b}^2$ if off-shell photon is allowed. In our case of $\Lambda_b \rightarrow \Lambda\gamma$, $q^2 = 0$. Here we have kept Λ mass in the expressions for the purpose in tracing the ranges of the kinematic variables. In the approximation we are using, it should be set to zero as mentioned above.

In the PQCD picture, hadrons are formed from quarks with appropriate wave functions describing the momenta distribution of quarks inside the hadron. The Λ_b wave function is usually defined through the quantity [18].

$$\begin{aligned} (Y_{\Lambda_b})_{\alpha\beta\gamma}(k_i, \nu) &= \frac{1}{2\sqrt{2}N_c} \int \prod_{l=2}^3 \frac{dw_l^+ d\mathbf{w}_l}{(2\pi)^3} e^{ik_l w_l} \varepsilon^{abc} \langle 0 | T [b_\alpha^a(0) u_\beta^b(w_2) d_\gamma^c(w_3)] | \Lambda_b(p) \rangle \\ &= \frac{f_{\Lambda_b}}{8\sqrt{2}N_c} [(\not{p} + M_{\Lambda_b})\gamma_5 C]_{\beta\gamma} [\Lambda_b(p)]_\alpha \Psi(k_i, \nu), \end{aligned} \quad (6)$$

where f_{Λ_b} is a normalization constant, $\Lambda_b(p)$ is the Λ_b spinor, and $\Psi(k_i, \mu)$ is the wave function. In a similar way the leading-twist wave function of Λ is defined by[19]:

$$\begin{aligned} (Y_\Lambda)_{\alpha\beta\gamma}(k'_i, \nu) &= \frac{1}{2\sqrt{2}N_c} \int \prod_{l=1}^2 \frac{dw_l^- d\mathbf{w}_l}{(2\pi)^3} e^{ik'_l w_l} \varepsilon^{abc} \langle 0 | T [s_\alpha^a(w_1) u_\beta^b(w_2) d_\gamma^c(0)] | \Lambda(p') \rangle \\ &= \frac{f_\Lambda}{8\sqrt{2}N_c} \{ (\not{p}' C)_{\beta\gamma} [\gamma_5 \Lambda(p')]_\alpha \Phi^V(k'_i, \nu) + (\not{p}' \gamma_5 C)_{\beta\gamma} [\Lambda(p')]_\alpha \Phi^A(k'_i, \nu) \} \\ &\quad - \frac{f_\Lambda^T}{8\sqrt{2}N_c} (\sigma_{\mu\nu} p'^\nu C)_{\beta\gamma} [\gamma^\mu \gamma_5 \Lambda(p')]_\alpha \Phi^T(k'_i, \nu), \end{aligned} \quad (7)$$

where f_Λ and f_Λ^T are normalization constants, and $\Lambda(p')$ is the Λ spinor.

Including the Sudakov factor with infrared cut-offs $\omega(\omega')$, and running the wavefunction from ν down to $\omega(\omega')$, then we obtain[13]:

$$\begin{aligned} \Psi(x_i, b_i, p, \nu) &= \exp\left[-\sum_{l=2}^3 s(\omega, x_l p^-) - 3 \int_\omega^\nu \frac{d\bar{\mu}}{\bar{\mu}} \gamma_q(\alpha_s(\bar{\mu}))\right] \Psi(x_i) \\ \Phi^j(x'_i, b'_i, p', \nu) &= \exp\left[-\sum_{l=1}^3 s(\omega', x'_l p^+) - 3 \int_{\omega'}^\nu \frac{d\bar{\mu}}{\bar{\mu}} \gamma_q(\alpha_s(\bar{\mu}))\right] \Phi^j(x'_i), \end{aligned} \quad (8)$$

where $j = V, A, T$, $\omega = \min(1/\tilde{b}_1, 1/\tilde{b}_2, 1/\tilde{b}_3)$, and $\omega' = \min(1/\tilde{b}'_1, 1/\tilde{b}'_2, 1/\tilde{b}'_3)$. $\tilde{b}_1^{(\prime)} = |\mathbf{b}_2^{(\prime)} - \mathbf{b}_3^{(\prime)}|$, $\tilde{b}_2^{(\prime)} = |\mathbf{b}_1^{(\prime)} - \mathbf{b}_3^{(\prime)}|$, and $\tilde{b}_3^{(\prime)} = |\mathbf{b}_1^{(\prime)} - \mathbf{b}_2^{(\prime)}|$. Here \mathbf{b} and \mathbf{b}' are the conjugate variables to \mathbf{k}_T and \mathbf{k}'_T defined in Appendix B.

The explicit expressions for the Sudakov factors are given in Ref.[13] with

$$\begin{aligned} s(\omega, Q) &= \int_\omega^Q \frac{dp}{p} \left[\ln\left(\frac{Q}{p}\right) A[\alpha_s(p)] + B[\alpha_s(p)] \right] \\ A &= C_F \frac{\alpha_s}{\pi} + \left[\frac{67}{9} - \frac{\pi^2}{3} - \frac{10}{27} n_f + \frac{8}{3} \beta_0 \ln\left(\frac{e^{\gamma_E}}{2}\right) \right] \left(\frac{\alpha_s}{\pi}\right)^2 \\ B &= \frac{2}{3} \frac{\alpha_s}{\pi} \ln\left(\frac{e^{2\gamma_E-1}}{2}\right) \\ \gamma_q(\alpha_s(\mu)) &= -\alpha_s(\mu)/\pi, \\ \beta_0 &= \frac{33 - 2n_f}{12}, \end{aligned} \quad (9)$$

where γ_E is the Euler constant. n_f is the flavor number, and γ_q is the anomalous dimension. For Λ_b baryon decays, the typical energy scale is above the charm mass. We will take n_f equal to 4 in our calculations.

The hadronic matrix elements can be written as:

$$M_{l,\mu} = \int [Dx] \int [Db] (\bar{Y}_\Lambda)_{\alpha'\beta'\gamma'}(x'_i, b'_i, p', \nu) H_{l,\mu}^{\alpha'\beta'\gamma'\alpha\beta\gamma}(x_i, x'_i, b_i, b'_i, M_{\Lambda_b}, \nu) (Y_{\Lambda_b})_{\alpha\beta\gamma}(x_i, b_i, p, \nu), \quad (10)$$

where the measures of the momentum fractions [13] are give by

$$[Dx] = [dx][dx'], \quad [dx] = dx_1 dx_2 dx_3 \delta(1 - \sum_{l=1}^3 x_l), \quad [dx'] = dx'_1 dx'_2 dx'_3 \delta(1 - \sum_{l=1}^3 x'_l). \quad (11)$$

The measures of the transverse extents $[Db]$ are defined in Appendix A.

The hard scattering amplitude $H_{l,\mu}^{\alpha'\beta'\gamma'\alpha\beta\gamma}(x, x', b, b', M_{\Lambda_b}, \nu)$ is obtained by first evaluating the amplitude $H_{l,\mu}^{i,\alpha'\beta'\gamma'\alpha\beta\gamma}(x_i, x'_i, \mathbf{k}_T, \mathbf{k}'_T, M_{\Lambda_b})$ for the 'i'th diagram in Fig. 1 for a corresponding Wilson coefficient C_l^{eff} which is displayed in Appendix B. One then carries out a Fourier transformation on \mathbf{k}_T and \mathbf{k}'_T to \vec{b} and \vec{b}' space to obtain $\tilde{H}_{l,\mu}^{i,\alpha'\beta'\gamma'\alpha\beta\gamma}(x, x', b, b', M_{\Lambda_b})$. The procedure of carrying out this transformation is described at the end of Appendix B.

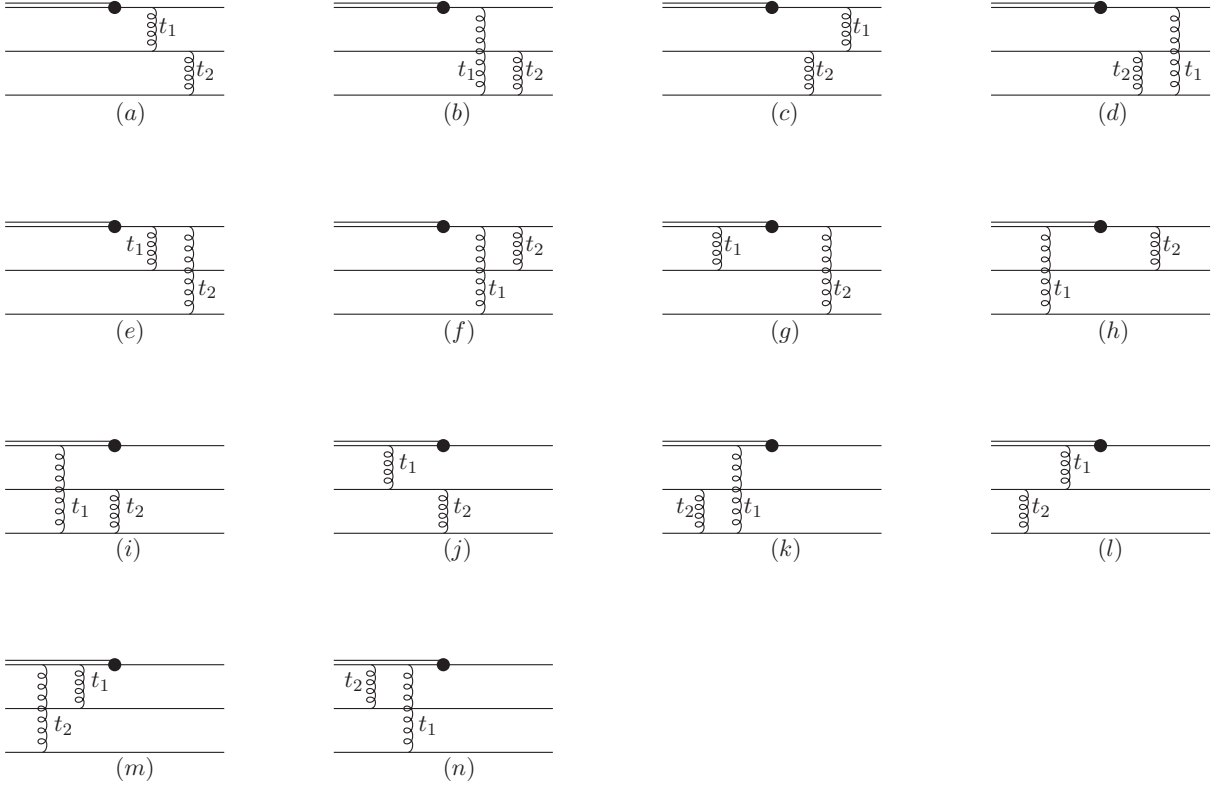


FIG. 1: The lowest order diagrams for the $\Lambda_b \rightarrow \Lambda \gamma$ decay. The solid lines, double lines, wavy lines and the black blue vertex denote the light quarks, b quark, gluon and the electromagnetic penguin vertex, respectively.

Collecting all contributions in Fig.1 and multiplying the corresponding Wilson coefficients, one then obtains a hard scattering amplitude $H_{l,\mu}^{\alpha'\beta'\gamma'\alpha\beta\gamma}(x, x', b, b', M_{\Lambda_b}) = \sum_i C_l^{eff}(t) \tilde{H}_{l,\mu}^{i,\alpha'\beta'\gamma'\alpha\beta\gamma}(x, x', b, b', M_{\Lambda_b})$. Here we have labelled the hard scale as t which is taken to be the larger of the two variables $t_{1,2}$ associated with the virtual gluon momentum in Fig. 1, i.e. $t = \max(t_1^i, t_2^i)$. The expressions for $t_{1,2}$ are listed in Appendix C.

Finally a RG running is applied to the hard scattering amplitude to match the scale ν in the wave functions and

we obtain[13]

$$H_{l,\mu}^{\alpha'\beta'\gamma'\alpha\beta\gamma}(x, x', b, b', M_{\Lambda_b}, \nu) = \exp[-6 \int_{\nu}^t \frac{d\bar{\mu}}{\bar{\mu}} \gamma_q(\alpha_s(\bar{\mu}))] \times H_{l,\mu}^{\alpha'\beta'\gamma'\alpha\beta\gamma}(x, x', b, b', M_{\Lambda_b}) \quad (12)$$

The form factors are obtained by grouping relevant terms according to the definition in eq. (3). Using eq.(10) we obtain a generic expression for the form factors corresponding to each diagram as

$$F_l^i = \sum_{j=V,A,T} \frac{\pi^2}{27} f_{\Lambda}^j f_{\Lambda_b} \int [Dx] \int [Db] {}^i C_l^{eff}(t^i) \Psi_{\Lambda_b}(x) \Phi_{\Lambda}^j(x') \exp[-S^i] H_F^{ij} \Omega^i$$

$$S = \sum_{k=2}^3 s(\omega, x_k p^-) + \sum_{k=1}^3 s(\omega', x'_k p'^+) + 3 \int_{\omega}^t \frac{d\bar{\mu}}{\bar{\mu}} \gamma_q(\alpha_s(\bar{\mu})) + 3 \int_{\omega'}^t \frac{d\bar{\mu}}{\bar{\mu}} \gamma_q(\alpha_s(\bar{\mu})) \quad (13)$$

where F_l^i represents the form factors contributed by the “i” the diagram in which operators with the Wilson coefficients C_l^{eff} are inserted, in our case $C_l^{eff} = C_7^{eff}$. The superscript j labels V, A , and T related to the spin structure of the valence quarks in the Λ baryon with $f_{\Lambda}^A = f_{\Lambda}^V = f_{\Lambda}$. The explicit expressions of Ω^i are presented in Appendix D. The functions H_F^{ij} are given in Appendix E. The total form factors are obtained by summing over contributions from all diagrams.

III. NUMERICAL RESULTS

We are now ready to evaluate the form factors numerically. For concreteness, we adopt the model proposed in Ref.[18] for the Λ_b baryon distribution amplitude Ψ ,

$$\Psi(x_1, x_2, x_3) = N x_1 x_2 x_3 \exp[-\frac{M_{\Lambda_b}^2}{2\beta^2 x_1} - \frac{m_q^2}{2\beta^2 x_2} - \frac{m_q^2}{2\beta^2 x_3}]. \quad (14)$$

The normalization constant N is obtained by the condition:

$$\int [dx] \Psi(x_1, x_2, x_3) = 1. \quad (15)$$

The decay constant f_{Λ_b} is determined in Ref.[14] to be $2.71 \times 10^{-3} \text{GeV}^2$.

The Λ baryon distribution amplitudes have been studied using QCD sum rules. In this work, we adopt the model proposed in Ref.[19],

$$\begin{aligned} \phi^V(x_1, x_2, x_3) &= 42\phi_{as}(x_1, x_2, x_3)[0.18(x_3^2 - x_2^2) + 0.10(x_2 - x_3)], \\ \phi^A(x_1, x_2, x_3) &= -42\phi_{as}(x_1, x_2, x_3)[0.26(x_3^2 + x_2^2) + 0.34x_1^2 - 0.56x_2x_3 - 0.24x_1(x_2 + x_3)], \\ \phi^T(x_1, x_2, x_3) &= 42\phi_{as}(x_1, x_2, x_3)[1.2(x_2^2 - x_3^2) - 1.4(x_2 - x_3)], \\ \phi_{as}(x_1, x_2, x_3) &= 120x_1x_2x_3. \end{aligned} \quad (16)$$

The asymmetric distribution in the momentum fractions of the three quarks implies $SU(3)$ symmetry breaking.

The constants f_{Λ} and f_{Λ}^T are fixed to be[19]

$$f_{\Lambda} = 0.63 \times 10^{-2} \text{GeV}^2, \quad f_{\Lambda}^T = 0.063 \times 10^{-2} \text{GeV}^2. \quad (17)$$

For definitiveness we fix the parameter Λ_{QCD} which enters in the strong coupling constant and various Wilson coefficients, the b quark mass, and the CKM mixing parameters to be: Λ_{QCD} at 0.2 GeV, $m_b = 4.8$ GeV, and use the central values in Ref.[20] for the CKM mixing parameters: $s_{12} = 0.2243$, $s_{23} = 0.00413$, $s_{13} = 0.0037$ and $\delta_{13} = 1.05$.

Moreover, β and m_q in the heavy baryon wavefunction distribution need to be fixed. In Ref.[13, 14, 15], $\beta = 1$ GeV and $m_q = 0.3$ GeV were used to estimate $\Lambda_b \rightarrow \Lambda_c l \bar{\nu}$, $\Lambda_b \rightarrow p l \bar{\nu}$ and also $\Lambda_b \rightarrow \Lambda J/\psi$ decays. β should not be too much smaller than 1 GeV if the form factors are dominated by perturbative contributions. Therefore we will let both β and m_q vary in the ranges $0.6 \sim 1$ GeV and $0.2 \sim 0.3$ GeV, respectively.

Our explicit calculations show that $F_L = 0$ and a non-zero value for F_R as expected since light quark and light baryon masses have been neglected. The contributions from each diagrams for F_R are shown in Appendix E. The resulting branching ratio is shown in Figure 2. We see that for reasonable ranges of parameters, the branching ratio can reach 1×10^{-7} .

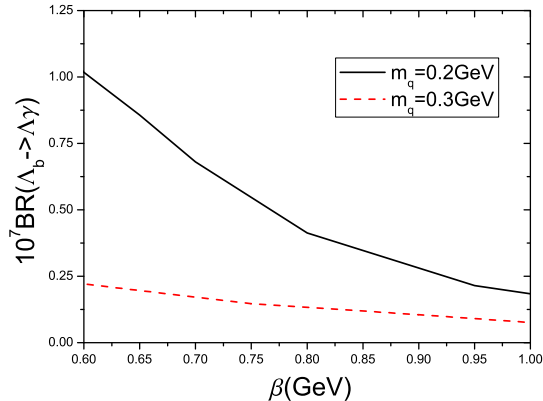


FIG. 2: $B(\Lambda_b \rightarrow \Lambda\gamma)$ as a function of β for different values for m_q .

IV. DISCUSSIONS AND CONCLUSIONS

In this work we have used the perturbative QCD approach to evaluate the branching ratio for radiative decay $\Lambda_b \rightarrow \Lambda\gamma$. This process occurs via penguin diagrams. Our results are shown in Figure 2. The branching ratio obtained is much smaller than results obtained, shown in Table I, using other methods.

TABLE I: Decay branching ratios (B) of $\Lambda_b \rightarrow \Lambda\gamma$ based on the form factors from the QCD sum rule approach, the covariant oscillator quark model, HQET and MIT bag model, respectively

Model	pole model[9]	QCD sum rule[10]	covariant oscillator quark model[11]	HQET[12]	bag model[12]
B	$(0.10 \sim 0.45) \times 10^{-5}$	$(3.7 \pm 0.5) \times 10^{-5}$	0.23×10^{-5}	$(1.2 \sim 1.9) \times 10^{-5}$	0.6×10^{-5}

There are uncertainties in PQCD predictions due to unknown parameters in wavefunctions. We have illustrated such uncertainties by varying relevant parameters. Within reasonable ranges of the parameters it is not possible to obtain large branching ratios listed in Table I. We have considered another possible uncertainty in the method used here. This is the choice of the infrared cut-offs $\omega(\omega')$ in the Sudakov suppression factor which damps the perturbative contributions. The cut-offs are set to the conventional values with $\omega = \min(1/\tilde{b}_1, 1/\tilde{b}_2, 1/\tilde{b}_3)$ and $\omega' = \min(1/\tilde{b}'_1, 1/\tilde{b}'_2, 1/\tilde{b}'_3)$ in previous discussions. In our opinion, these are just convenient values to choose. But the fact may be different from this case. We have therefore tried to see how sensitive the results depend on the choice of the cut-offs. The smaller these values are the more severe the Sudakov suppression effects are. It turns out that the branching ratios are very sensitive to the choice. For example with $\beta = 1$ GeV, $m_q = 0.3$ GeV, $\omega = 2\min(1/\tilde{b}_1, 1/\tilde{b}_2, 1/\tilde{b}_3)$, and $\omega' = 2\min(1/\tilde{b}'_1, 1/\tilde{b}'_2, 1/\tilde{b}'_3)$, one would obtain $B(\Lambda_b \rightarrow \Lambda\gamma) = 1.5 \times 10^{-7}$, whereas with the conventional cut-off the branching ratio is 2×10^{-9} . This sensitivity on the infrared cut-offs casts some doubts on the method. However since this theoretical framework well describes the B meson decays, it is reasonable to believe that it should apply to the baryon case at least for an order of magnitude estimate. One still cannot rule out the case that the non-perturbative QCD effects should dominate in certain baryon decay modes. We do not have a definite answer yet. But estimate for $\Lambda_b \rightarrow \Lambda J/\psi$ using the same method gives a reasonable range compared with data[15], a choice of the cut-off with a large deviation from the conventional one may not be a good direction to go.

If the conventional choice of the infrared cut-offs in the Sudakov suppression is the correct choice, the branching ratio for $\Lambda_b \rightarrow \Lambda\gamma$ is smaller than other model calculations. The agreement of $\Lambda_b \rightarrow \Lambda J/\psi$ using the same method indicates that our choice is a reasonable one. We conclude that PQCD prediction for $\Lambda_b \rightarrow \Lambda\gamma$ is smaller than predictions using other methods listed in Table I. Future experiments can test the PQCD prediction.

The small branching ratio makes it phenomenologically difficult to obtain information about the SM contributions to $\Lambda_b \rightarrow \Lambda\gamma$. However this may be a good thing for the study of beyond the SM effects. Should a larger branching ratio is measured for $\Lambda_b \rightarrow \Lambda\gamma$, it may be an indication of new physics beyond the SM. We have to wait for more data to come to give an answer.

Acknowledgements:

This work is supported by NNSFC and NSC. We would like to thank Hsiang-nan Li and Cai-Dian Lü for helpful discussions. We also thank H.n. Li for providing us with the program for numerical integration.

Appendix A: the b measures

The ordinary b measure is defined as

$$[d\mathbf{b}] = \frac{d^2\mathbf{b}}{(2\pi)^2} \quad (18)$$

The explicit forms of $[D\mathbf{b}]^i$ for each diagram i in Fig. 1 are given by

$$\begin{aligned} [D\mathbf{b}]^{(a)} &= [d\mathbf{b}_1][d\mathbf{b}_3][d\mathbf{b}'_1][d\mathbf{b}'_3], & [D\mathbf{b}]^{(b)} &= [d\mathbf{b}_1][d\mathbf{b}_2][d\mathbf{b}'_1][d\mathbf{b}'_2], \\ [D\mathbf{b}]^{(c)} &= [d\mathbf{b}_1][d\mathbf{b}_3][d\mathbf{b}'_1][d\mathbf{b}'_3], & [D\mathbf{b}]^{(d)} &= [d\mathbf{b}_1][d\mathbf{b}_2][d\mathbf{b}'_1][d\mathbf{b}'_2], \\ [D\mathbf{b}]^{(e)} &= [d\mathbf{b}_2][d\mathbf{b}'_2][d\mathbf{b}'_3], & [D\mathbf{b}]^{(f)} &= [d\mathbf{b}_3][d\mathbf{b}'_2][d\mathbf{b}'_3], \\ [D\mathbf{b}]^{(g)} &= [d\mathbf{b}_2][d\mathbf{b}_3][d\mathbf{b}'_3], & [D\mathbf{b}]^{(h)} &= [d\mathbf{b}_2][d\mathbf{b}_3][d\mathbf{b}'_2], \\ [D\mathbf{b}]^{(i)} &= [d\mathbf{b}_1][d\mathbf{b}_2][d\mathbf{b}'_1][d\mathbf{b}'_2], & [D\mathbf{b}]^{(j)} &= [d\mathbf{b}_1][d\mathbf{b}_3][d\mathbf{b}'_1][d\mathbf{b}'_3], \\ [D\mathbf{b}]^{(k)} &= [d\mathbf{b}_1][d\mathbf{b}_2][d\mathbf{b}'_1][d\mathbf{b}'_2], & [D\mathbf{b}]^{(l)} &= [d\mathbf{b}_1][d\mathbf{b}_3][d\mathbf{b}'_1][d\mathbf{b}'_3], \\ [D\mathbf{b}]^{(m)} &= [d\mathbf{b}_2][d\mathbf{b}_3][d\mathbf{b}'_2], & [D\mathbf{b}]^{(n)} &= [d\mathbf{b}_2][d\mathbf{b}_3][d\mathbf{b}'_3]. \end{aligned} \quad (19)$$

Appendix B: Hard scattering amplitudes $H_{l,\mu}^{i,\alpha'\beta'\gamma'\alpha\beta\gamma}(x_i, x'_i, \mathbf{k}_T, \mathbf{k}'_T, M_{\Lambda_b})$

Expressions of amplitude $H_{l,\mu}^{i,\alpha'\beta'\gamma'\alpha\beta\gamma}(x_i, x'_i, \mathbf{k}_T, \mathbf{k}'_T, M_{\Lambda_b})$ for each diagram in Fig. 1. In the following O'_μ comes from the γ -matrix in the effective Hamiltonian, $O_\mu^{l=7} = \sigma_{\mu\nu}q^\nu R$

For the hard amplitude of Fig.1(a):

$$\begin{aligned} H_\mu^{a,\alpha'\beta'\gamma'\alpha\beta\gamma}(x_i, x'_i, \mathbf{k}_T, \mathbf{k}'_T, M_{\Lambda_b}) &= \\ & [\varepsilon^{abc}\varepsilon^{a'b'c'}(T^j)_{c'c}(T^jT^i)_{b'b}(T^i)_{a'a}]g_s^4 \frac{(\gamma_\rho)_{\gamma'\gamma}[\gamma^\rho(\not{p}' - \not{k}'_1 - \not{k}_3)\gamma^\lambda]_{\beta'\beta}[\gamma_\lambda(\not{p}' - \not{p} + \not{k}_1)O_\mu]_{\alpha'\alpha}}{(p' - k'_1 - k_3)^2(p' - p + k_1)^2(p - p' + k'_1 - k_1)^2(k_3 - k'_3)^2} \\ &= C_N g_s^4 \frac{(\gamma_\rho)_{\gamma'\gamma}[\gamma^\rho(\not{p}' - \not{k}'_1 - \not{k}_3)\gamma^\lambda]_{\beta'\beta}[\gamma_\lambda(\not{p}' - \not{p} + \not{k}_1)O_\mu]_{\alpha'\alpha}}{[A_a + (\mathbf{k}'_{1T} + \mathbf{k}_{3T})^2][B_a + \mathbf{k}_{1T}^2][C_a + (\mathbf{k}_{1T} - \mathbf{k}'_{1T})^2][D_a + (\mathbf{k}_{3T} - \mathbf{k}'_{3T})^2]} \end{aligned} \quad (20)$$

with

$$A_a = x_3(1 - x'_1)\rho M_{\Lambda_b}^2, B_a = (1 - x_1)\rho M_{\Lambda_b}^2, C_a = (1 - x_1)(1 - x'_1)\rho M_{\Lambda_b}^2, D_a = x_3x'_3\rho M_{\Lambda_b}^2 \quad (21)$$

and the color factor

$$C_N = \varepsilon^{abc}\varepsilon^{a'b'c'}(T^j)_{c'c}(T^jT^i)_{b'b}(T^i)_{a'a} = \frac{(N^2 - 1)(N + 1)}{12} \quad (22)$$

For the hard amplitude of Fig.1(b):

$$\begin{aligned} H_\mu^{b,\alpha'\beta'\gamma'\alpha\beta\gamma}(x_i, x'_i, \mathbf{k}_T, \mathbf{k}'_T, M_{\Lambda_b}) &= \\ & [\varepsilon^{abc}\varepsilon^{a'b'c'}(T^i)_{c'c}(T^i)_{b'b}(T^j)_{a'a}]g_s^4 \frac{(\gamma^\rho)_{\beta'\beta}[\gamma_\rho(\not{p}' - \not{k}'_1 - \not{k}_2)\gamma_\lambda]_{\gamma'\gamma}[\gamma^\lambda(\not{p}' - \not{p} + \not{k}_1)O_\mu]_{\alpha'\alpha}}{(p' - k'_1 - k_2)^2(p' - p + k_1)^2(p - p' - k_1 + k'_1)^2(k'_2 - k_2)^2} \\ &= C_N g_s^4 \frac{(\gamma^\rho)_{\beta'\beta}[\gamma_\rho(\not{p}' - \not{k}'_1 - \not{k}_2)\gamma_\lambda]_{\gamma'\gamma}[\gamma^\lambda(\not{p}' - \not{p} + \not{k}_1)O_\mu]_{\alpha'\alpha}}{[A_b + (\mathbf{k}'_{1T} + \mathbf{k}_{2T})^2][B_b + \mathbf{k}_{1T}^2][C_b + (\mathbf{k}_{1T} - \mathbf{k}'_{1T})^2][D_b + (\mathbf{k}_{2T} - \mathbf{k}'_{2T})^2]} \end{aligned} \quad (23)$$

with

$$A_b = x_2(1 - x'_1)\rho M_{\Lambda_b}^2, B_b = (1 - x_1)\rho M_{\Lambda_b}^2, C_b = (1 - x_1)(1 - x'_1)\rho M_{\Lambda_b}^2, D_b = x_2x'_2\rho M_{\Lambda_b}^2 \quad (24)$$

Inspection of the above calculations, one notices that one can easily obtain $H_\mu^{b,\alpha'\beta'\gamma'\alpha\beta\gamma}(x_i, x'_i, \mathbf{k}_T, \mathbf{k}'_T, M_{\Lambda_b})$ from $H_\mu^{a,\alpha'\beta'\gamma'\alpha\beta\gamma}(x_i, x'_i, \mathbf{k}_T, \mathbf{k}'_T, M_{\Lambda_b})$ and vice versa by simply exchanging the momentum indices 2 and 3 for \mathbf{k} and \mathbf{k}' ,

and exchanging the positions of the Dirac indices $\gamma'\gamma$ and $\beta'\beta$. Due to these properties, the contributions to the form factors from the above two diagrams are the same. This fact can be easily understood by noticing the following properties of the quantities related to the distribution amplitudes: i) The distribution amplitudes $\Psi(x_1, x_2, x_3)$, and $\phi^A(x_1, x_2, x_3)$ are symmetric in exchanging x_2 and x_3 , while $\phi^{V,T}(x_1, x_2, x_3)$ are anti-symmetric in exchanging x_2 and x_3 , as can be seen from eqs.(14) and (16). And ii) When exchanging the Dirac indices β and γ , the expressions for $(Y_{\Lambda_b})_{\alpha\beta\gamma}(k_i\nu)$ in eq.(6), and terms proportional to ϕ^A for $(Y_{\Lambda})_{\alpha\beta\gamma}(k'_i, \nu)$ in eq.(7) will have a sign change, while terms proportional to $\phi^{V,T}$ remain the same. Since going from the contribution of diagram (a) to diagram (b) involves both actions: exchanging the momentum indices 2 and 3, and the Dirac indices β and γ , this results in no sign changes for all the terms involved. After integrating out $x(x')_{2,3}$ and $b(b')_{2,3}$ to obtain the final form factors using eq.(13), one then obtains the same results for both diagrams (a) and (b).

Similar situation happens for the following pairs of diagrams: (c) and (d), (e) and (f), (g) and (h), (i) and (j), (k) and (l), and, (m) and (n). In the following we will only display the results for diagrams (a), (c), (e), (g), (i), (k) and (m). The expressions for diagrams (b), (d), (f), (h), (j), (l) and (n) can be obtained by exchanging $x(x')_2$ and $x(x')_3$, and also $\gamma'\gamma$ and $\beta'\beta$.

For the hard amplitude of Fig.1(c):

$$\begin{aligned} H_{\mu}^{c,\alpha'\beta'\gamma'\alpha\beta\gamma}(x_i, x'_i, \mathbf{k}_T, \mathbf{k}'_T, M_{\Lambda_b}) &= \\ [\varepsilon^{abc}\varepsilon^{a'b'c'}(T^j)_{c'c}(T^iT^j)_{b'b}(T^i)_{a'a}]g_s^4 &\frac{(\gamma_{\rho})_{\gamma'\gamma}[\gamma^{\lambda}(\not{p}-\not{k}_1-\not{k}'_3)\gamma^{\rho}]_{\beta'\beta}[\gamma_{\lambda}(\not{p}'-\not{p}+\not{k}_1)O_{\mu}]_{\alpha'\alpha}}{(p-k_1-k'_3)^2(p'-p+k_1)^2(p-p'+k'_1-k_1)^2(k_3-k'_3)^2} \\ &= C_N g_s^4 \frac{(\gamma_{\rho})_{\gamma'\gamma}[\gamma^{\lambda}(\not{p}-\not{k}_1-\not{k}'_3)\gamma^{\rho}]_{\beta'\beta}[\gamma_{\lambda}(\not{p}'-\not{p}+\not{k}_1)O_{\mu}]_{\alpha'\alpha}}{[A_c + (\mathbf{k}_{1T} + \mathbf{k}'_{3T})^2][B_c + \mathbf{k}_{1T}^2][C_c + (\mathbf{k}_{3T} - \mathbf{k}'_{3T})^2][D_c + (\mathbf{k}_{1T} - \mathbf{k}'_{1T})^2]} \end{aligned} \quad (25)$$

with

$$A_c = x'_3(1-x_1)\rho M_{\Lambda_b}^2, B_c = (1-x_1)\rho M_{\Lambda_b}^2, C_c = x_3x'_3\rho M_{\Lambda_b}^2, D_c = (1-x_1)(1-x'_1)\rho M_{\Lambda_b}^2 \quad (26)$$

For the hard amplitude of Fig.1(e):

$$\begin{aligned} H_{\mu}^{e,\alpha'\beta'\gamma'\alpha\beta\gamma}(x_i, x'_i, \mathbf{k}_T, \mathbf{k}'_T, M_{\Lambda_b}) &= \\ [\varepsilon^{abc}\varepsilon^{a'b'c'}(T^i)_{c'c}(T^iT^j)_{b'b}(T^j)_{a'a}]g_s^4 &\frac{(\gamma_{\rho})_{\gamma'\gamma}[\gamma^{\rho}(\not{p}'-\not{k}'_2-\not{k}_3)\gamma^{\lambda}(\not{p}'-\not{p}+\not{k}_1)O_{\mu}]_{\alpha'\alpha}(\gamma_{\lambda})_{\beta'\beta}}{(p'-k'_2-k_3)^2(p'-p+k_1)^2(k'_2-k_2)^2(k_3-k'_3)^2} \\ &= C_N g_s^4 \frac{(\gamma_{\rho})_{\gamma'\gamma}[\gamma^{\rho}(\not{p}'-\not{k}'_2-\not{k}_3)\gamma^{\lambda}(\not{p}'-\not{p}+\not{k}_1)O_{\mu}]_{\alpha'\alpha}(\gamma_{\lambda})_{\beta'\beta}}{[A_e + (\mathbf{k}'_{2T} + \mathbf{k}_{3T})^2][B_e + \mathbf{k}'_{1T}{}^2][C_e + (\mathbf{k}_{2T} - \mathbf{k}'_{2T})^2][D_e + (\mathbf{k}_{3T} - \mathbf{k}'_{3T})^2]} \end{aligned} \quad (27)$$

with

$$A_e = x_3(1-x'_1)\rho M_{\Lambda_b}^2, B_e = (1-x_1)\rho M_{\Lambda_b}^2, C_e = x_2x'_2\rho M_{\Lambda_b}^2, D_e = x_3x'_3\rho M_{\Lambda_b}^2 \quad (28)$$

For the hard amplitude of Fig.1(g):

$$\begin{aligned} H_{\mu}^{g,\alpha'\beta'\gamma'\alpha\beta\gamma}(x_i, x'_i, \mathbf{k}_T, \mathbf{k}'_T, M_{\Lambda_b}) &= \\ [\varepsilon^{abc}\varepsilon^{a'b'c'}(T^i)_{c'c}(T^j)_{b'b}(T^iT^j)_{a'a}]g_s^4 &\frac{(\gamma_{\rho})_{\gamma'\gamma}[\gamma^{\rho}(\not{p}'-\not{k}'_2-\not{k}_3)O_{\mu}(\not{p}-\not{k}_3-\not{k}'_2+m_b)\gamma^{\lambda}]_{\alpha'\alpha}(\gamma_{\lambda})_{\beta'\beta}}{[(p-k_3-k'_2)^2-m_b^2](p'-k'_2-k_3)^2(k'_2-k_2)^2(k'_3-k_3)^2} \\ &= C_N g_s^4 \frac{(\gamma_{\rho})_{\gamma'\gamma}[\gamma^{\rho}(\not{p}'-\not{k}'_2-\not{k}_3)O_{\mu}(\not{p}-\not{k}_3-\not{k}'_2+m_b)\gamma^{\lambda}]_{\alpha'\alpha}(\gamma_{\lambda})_{\beta'\beta}}{[A_g + (\mathbf{k}'_{2T} + \mathbf{k}_{3T})^2][B_g + (\mathbf{k}'_{2T} + \mathbf{k}_{3T})^2][C_g + (\mathbf{k}_{2T} - \mathbf{k}'_{2T})^2][D_g + (\mathbf{k}_{3T} - \mathbf{k}'_{3T})^2]} \end{aligned} \quad (29)$$

with

$$A_g = (x'_2(1-x_3)\rho + x_3)M_{\Lambda_b}^2, B_g = x_3(1-x'_2)\rho M_{\Lambda_b}^2, C_g = x_2x'_2\rho M_{\Lambda_b}^2, D_g = x_3x'_3\rho M_{\Lambda_b}^2 \quad (30)$$

For the hard amplitude of Fig.1(i):

$$\begin{aligned} H_{\mu}^{i,\alpha'\beta'\gamma'\alpha\beta\gamma}(x_i, x'_i, \mathbf{k}_T, \mathbf{k}'_T, M_{\Lambda_b}) &= \\ [\varepsilon^{abc}\varepsilon^{a'b'c'}(T^iT^j)_{c'c}(T^i)_{b'b}(T^j)_{a'a}]g_s^4 &\frac{[\gamma_{\rho}(\not{p}'-\not{k}'_1-\not{k}_2)\gamma_{\lambda}]_{\gamma'\gamma}[O_{\mu}(\not{p}-\not{p}'-\not{k}'_1+m_b)\gamma^{\lambda}]_{\alpha'\alpha}(\gamma^{\rho})_{\beta'\beta}}{[(p-p'+k'_1)^2-m_b^2](p'-k'_1-k_2)^2(p-p'-k_1+k'_1)^2(k'_2-k_2)^2} \\ &= C_N g_s^4 \frac{[\gamma_{\rho}(\not{p}'-\not{k}'_1-\not{k}_2)\gamma_{\lambda}]_{\gamma'\gamma}[O_{\mu}(\not{p}-\not{p}'-\not{k}'_1+m_b)\gamma^{\lambda}]_{\alpha'\alpha}(\gamma^{\rho})_{\beta'\beta}}{[A_i + (\mathbf{k}_{2T} + \mathbf{k}'_{1T})^2][B_i + (\mathbf{k}'_{1T} + \mathbf{k}_{2T})^2][C_i + (\mathbf{k}_{1T} - \mathbf{k}'_{1T})^2][D_i + (\mathbf{k}_{2T} - \mathbf{k}'_{2T})^2]} \end{aligned} \quad (31)$$

with

$$A_i = (1 - x'_1)\rho M_{\Lambda_b}^2, B_i = x_2(1 - x'_1)\rho M_{\Lambda_b}^2, C_i = (1 - x_1)(1 - x'_1)\rho M_{\Lambda_b}^2, D_i = x_2x'_2\rho M_{\Lambda_b}^2 \quad (32)$$

For the hard amplitude of Fig.1(k):

$$\begin{aligned} H_\mu^{k,\alpha'\beta'\gamma'\alpha\beta\gamma}(x_i, x'_i, \mathbf{k}_T, \mathbf{k}'_T, M_{\Lambda_b}) &= \\ & [\varepsilon^{abc}\varepsilon^{a'b'c'}(T^iT^j)_{c'c}(T^j)_{b'b}(T^i)_{a'a}]g_s^4 \frac{[\gamma_\rho(\not{p} - \not{k}_1 - \not{k}'_2)\gamma_\lambda]_{\gamma'\gamma}[O_\mu(\not{p} - \not{p}' + \not{k}'_1 + m_b)\gamma^\rho]_{\alpha'\alpha}(\gamma^\lambda)_{\beta'\beta}}{[(p - p' + k'_1)^2 - m_b^2](p - k_1 - k'_2)^2(p - p' - k_1 + k'_1)^2(k'_2 - k_2)^2} \\ &= C_N g_s^4 \frac{[\gamma_\rho(\not{p} - \not{k}_1 - \not{k}'_2)\gamma_\lambda]_{\gamma'\gamma}[O_\mu(\not{p} - \not{p}' + \not{k}'_1 + m_b)\gamma^\rho]_{\alpha'\alpha}(\gamma^\lambda)_{\beta'\beta}}{[A_k + \mathbf{k}_{1T}^2][B_k + (\mathbf{k}_{1T} + \mathbf{k}'_{2T})^2][C_k + (\mathbf{k}_{1T} - \mathbf{k}'_{1T})^2][D_k + (\mathbf{k}_{2T} - \mathbf{k}'_{2T})^2]} \end{aligned} \quad (33)$$

with

$$A_k = (1 - x'_1)\rho M_{\Lambda_b}^2, B_k = x'_2(1 - x_1)\rho M_{\Lambda_b}^2, C_k = (1 - x_1)(1 - x'_1)\rho M_{\Lambda_b}^2, D_k = x_2x'_2\rho M_{\Lambda_b}^2 \quad (34)$$

For the hard amplitude of Fig.1(m):

$$\begin{aligned} H_\mu^{m,\alpha'\beta'\gamma'\alpha\beta\gamma}(x_i, x'_i, \mathbf{k}_T, \mathbf{k}'_T, M_{\Lambda_b}) &= \\ & [\varepsilon^{abc}\varepsilon^{a'b'c'}(T^j)_{c'c}(T^i)_{b'b}(T^i T^j)_{a'a}]g_s^4 \frac{(\gamma_\lambda)_{\gamma'\gamma}[O_\mu(\not{p} - \not{p}' + \not{k}'_1 + m_b)\gamma_\rho(\not{p} - \not{k}_2 - \not{k}'_3 + m_b)\gamma^\lambda]_{\alpha'\alpha}(\gamma^\rho)_{\beta'\beta}}{[(p - p' + k'_1)^2 - m_b^2][(p - k_2 - k'_3)^2 - m_b^2](k'_2 - k_2)^2(k'_3 - k_3)^2} \\ &= C_N g_s^4 \frac{(\gamma_\lambda)_{\gamma'\gamma}[O_\mu(\not{p} - \not{p}' + \not{k}'_1 + m_b)\gamma_\rho(\not{p} - \not{k}_2 - \not{k}'_3 + m_b)\gamma^\lambda]_{\alpha'\alpha}(\gamma^\rho)_{\beta'\beta}}{[A_m + \mathbf{k}_{1T}^2][B_m + (\mathbf{k}_{2T} + \mathbf{k}'_{3T})^2][C_m + (\mathbf{k}_{2T} - \mathbf{k}'_{2T})^2][D_m + (\mathbf{k}_{3T} - \mathbf{k}'_{3T})^2]} \end{aligned} \quad (35)$$

with

$$A_m = (1 - x'_1)\rho M_{\Lambda_b}^2, B_m = (x'_3(1 - x_2)\rho + x_2)M_{\Lambda_b}^2, C_m = x_2x'_2\rho M_{\Lambda_b}^2, D_m = x_3x'_3\rho M_{\Lambda_b}^2 \quad (36)$$

The expressions for the hard scattering amplitude in b and b' space are obtained by making a Fourier transformation on k_T and k'_T space. In the following we give one example for Fig.1(a) as an illustration. We note that the k_T and k'_T dependencies are all in the denominators in the above expressions, one then just needs to consider that part of the fourier transformation. For Fig.1(a), it is given by

$$\Omega^{(a)}(x_i, x'_i, \mathbf{k}_T, \mathbf{k}'_T, M_{\Lambda_b}) = \frac{1}{[A_a + (\mathbf{k}'_{1T} + \mathbf{k}_{3T})^2][B_a + \mathbf{k}_{1T}^2][C_a + (\mathbf{k}_{1T} - \mathbf{k}'_{1T})^2][D_a + (\mathbf{k}_{3T} - \mathbf{k}'_{3T})^2]} \quad (37)$$

The fourier transformed expression is then given by

$$\Omega^{(a)}(x_i, x'_i, b_i, b'_i, M_{\Lambda_b}) = \int e^{-i(\mathbf{k}_{1T}\cdot\mathbf{b}_1 + \mathbf{k}'_{1T}\cdot\mathbf{b}'_1 + \mathbf{k}_{3T}\cdot\mathbf{b}_3 + \mathbf{k}'_{3T}\cdot\mathbf{b}'_3)} \Omega^{(a)}(x_i, x'_i, \mathbf{k}_T, \mathbf{k}'_T, M_{\Lambda_b}) d^2\mathbf{k}_{1T} d^2\mathbf{k}'_{1T} d^2\mathbf{k}_{3T} d^2\mathbf{k}'_{3T}. \quad (38)$$

Defining $\mathbf{k}_{AT} \equiv \mathbf{k}'_{1T} + \mathbf{k}_{3T}$, $\mathbf{k}_{BT} \equiv \mathbf{k}_{1T}$, $\mathbf{k}_{CT} \equiv \mathbf{k}_{1T} - \mathbf{k}'_{1T}$, and $\mathbf{k}_{DT} \equiv \mathbf{k}_{3T} - \mathbf{k}'_{3T}$, we rewrite the transformation as

$$\begin{aligned} & \Omega^{(a)}(x_i, x'_i, b_i, b'_i, M_{\Lambda_b}) \\ &= \int \frac{e^{-i[\mathbf{k}_{AT}\cdot(\mathbf{b}_3 + \mathbf{b}'_3) + \mathbf{k}_{BT}\cdot(\mathbf{b}_1 + \mathbf{b}'_1 - \mathbf{b}_3 - \mathbf{b}'_3) + \mathbf{k}_{CT}\cdot(-\mathbf{b}'_1 + \mathbf{b}_3 + \mathbf{b}'_3) + \mathbf{k}_{DT}\cdot(-\mathbf{b}'_3)]}}{(\mathbf{k}_{AT}^2 + A_a)(\mathbf{k}_{BT}^2 + B_a)(\mathbf{k}_{CT}^2 + C_a)(\mathbf{k}_{DT}^2 + D_a)} d^2\mathbf{k}_{AT} d^2\mathbf{k}_{BT} d^2\mathbf{k}_{CT} d^2\mathbf{k}_{DT} \\ &= (2\pi)^4 K_0(\sqrt{A_a}|b_3 + b'_3|) K_0(\sqrt{B_a}|b_1 + b'_1 - b_3 - b'_3|) K_0(\sqrt{C_a}|b'_1 - b_3 - b'_3|) K_0(\sqrt{D_a}|b'_3|), \end{aligned} \quad (39)$$

In the above we have used

$$\int d^2k \frac{e^{i\mathbf{k}\cdot\mathbf{b}}}{k^2 + A} = 2\pi K_0(\sqrt{A}|\mathbf{b}|), A > 0. \quad (40)$$

One obtains the expression for $H_\mu^{a,\alpha'\beta'\gamma'\alpha\beta\gamma}(x_i, x'_i, b, b', M_{\Lambda_b})$ as

$$H_\mu^{a,\alpha'\beta'\gamma'\alpha\beta\gamma}(x_i, x'_i, b, b', M_{\Lambda_b}) = C_N g_s^4 (\gamma_\rho)_{\gamma'\gamma} [\gamma^\rho(\not{p}' - \not{k}'_1 - \not{k}_3)\gamma^\lambda]_{\beta'\beta} [\gamma_\lambda(\not{p}' - \not{p} + \not{k}_1)O_\mu]_{\alpha'\alpha} \widetilde{\Omega}^{(a)}(x_i, x'_i, b_i, b'_i, M_{\Lambda_b}). \quad (41)$$

In carrying out the fourier transformations for other diagrams, two other forms of functions will be encountered. We list them in the following

$$\int d^2k \frac{e^{i\mathbf{k}\cdot\mathbf{b}}}{(k^2 + A)(k^2 + B)} = \pi \int_0^1 dz \frac{|\mathbf{b}|K_1(\sqrt{Z_1}|\mathbf{b}|)}{\sqrt{Z_1}}, A, B > 0,$$

$$\int d^2k_1 d^2k_2 \frac{e^{i(\mathbf{k}_1\cdot\mathbf{b}_1 + \mathbf{k}_2\cdot\mathbf{b}_2)}}{(k_1^2 + A)(k_2^2 + B)[(k_1 + k_2)^2 + C]} = \pi^2 \int_0^1 \frac{dz_1 dz_2}{z_1(1-z_1)} \frac{\sqrt{X_2}}{\sqrt{|Z_2|}} K_1(\sqrt{X_2 Z_2}), \quad (42)$$

where $A > 0$ and B, C arbitrary. K_0 and K_1 are the modified Bessel functions of the second kind. And

$$Z_1 = Az + B(1-z),$$

$$Z_2 = A(1-z_2) + \frac{z_2}{z_1(1-z_1)}[B(1-z_1) + Cz_1],$$

$$X_2 = (\mathbf{b}_1 - z_1\mathbf{b}_2)^2 + \frac{z_1(1-z_1)}{z_2}\mathbf{b}_2^2 \quad (43)$$

Appendix C: The maximum of $t_{1,2}$

The hard scales, the maximal of t_1^i and t_2^i for diagrams (a), (c), (e), (g), (i), (k), and (m) in Fig. 1. Exchanging $b(b')_2$ and $b(b')_3$, one obtains the expressions for diagrams (b), (d), (f), (h), (j), (l) and (n). The expressions of C_i, D_i are collected in Appendix B.

i	t_1^i	t_2^i
(a)	$\max\{\sqrt{ C_a }, \frac{1}{ \mathbf{b}'_1 - \mathbf{b}_3 - \mathbf{b}'_3 }, \omega, \omega'\}$	$\max\{\sqrt{ D_a }, \frac{1}{ \mathbf{b}'_3 }, \omega, \omega'\}$
(c)	$\max\{\sqrt{ C_c }, \frac{1}{ \mathbf{b}'_1 }, \omega, \omega'\}$	$\max\{\sqrt{ D_c }, \frac{1}{ \mathbf{b}'_3 }, \omega, \omega'\}$
(e)	$\max\{\sqrt{ C_e }, \frac{1}{ \mathbf{b}'_2 }, \omega, \omega'\}$	$\max\{\sqrt{ D_e }, \frac{1}{ \mathbf{b}'_3 }, \omega, \omega'\}$
(g)	$\max\{\sqrt{ C_g }, \frac{1}{ \mathbf{b}'_2 }, \omega, \omega'\}$	$\max\{\sqrt{ D_g }, \frac{1}{ \mathbf{b}'_3 }, \omega, \omega'\}$
(i)	$\max\{\sqrt{ C_i }, \frac{1}{ \mathbf{b}'_1 }, \omega, \omega'\}$	$\max\{\sqrt{ D_i }, \frac{1}{ \mathbf{b}'_2 }, \omega, \omega'\}$
(k)	$\max\{\sqrt{ C_k }, \frac{1}{ \mathbf{b}_1 - \mathbf{b}_2 - \mathbf{b}'_2 }, \omega, \omega'\}$	$\max\{\sqrt{ D_k }, \frac{1}{ \mathbf{b}'_2 }, \omega, \omega'\}$
(m)	$\max\{\sqrt{ C_m }, \frac{1}{ \mathbf{b}'_2 }, \omega, \omega'\}$	$\max\{\sqrt{ D_m }, \frac{1}{ \mathbf{b}'_3 }, \omega, \omega'\}$

Appendix D: Expressions of Ω^i

The expression of Ω^i for diagrams (a), (c), (e), (g), (i), (k), and (m) in Fig. 1. Exchanging $b(b')_2$ and $b(b')_3$, one obtains the expressions for diagrams (b), (d), (f), (h), (j), (l) and (n).

$$\Omega^{(a)} = (2\pi)^4 K_0(\sqrt{A_a}|\mathbf{b}_3 + \mathbf{b}'_3|)K_0(\sqrt{B_a}|\mathbf{b}_1 + \mathbf{b}'_1 - \mathbf{b}_3 - \mathbf{b}'_3|)K_0(\sqrt{C_a}|\mathbf{b}'_1 - \mathbf{b}_3 - \mathbf{b}'_3|)K_0(\sqrt{D_a}|\mathbf{b}'_3|)$$

$$\Omega^{(c)} = (2\pi)^4 K_0(\sqrt{A_c}|\mathbf{b}_3 + \mathbf{b}'_3|)K_0(\sqrt{B_c}|\mathbf{b}_1 + \mathbf{b}'_1 + \mathbf{b}_3 + \mathbf{b}'_3|)K_0(\sqrt{C_c}|\mathbf{b}'_1|)K_0(\sqrt{D_c}|\mathbf{b}_3|)$$

$$\Omega^{(e)} = 8\pi^5 \int_0^1 dz_1 dz_2 \frac{1}{z_1(1-z_1)} \frac{\sqrt{X_2^e}}{\sqrt{|Z_2^e|}} K_1(\sqrt{X_2^e Z_2^e}) K_0(\sqrt{D_e}|\mathbf{b}'_3|)$$

$$\Omega^{(g)} = 16\pi^5 \int_0^1 dz \frac{|\mathbf{b}_3 + \mathbf{b}'_3|K_1(\sqrt{Z_1^g}|\mathbf{b}_3 + \mathbf{b}'_3|)}{\sqrt{Z_1^g}} K_0(\sqrt{C_g}|\mathbf{b}_2|)K_0(\sqrt{D_g}|\mathbf{b}'_3|)$$

$$\Omega^{(i)} = (2\pi)^4 K_0(\sqrt{A_i}|\mathbf{b}_1 + \mathbf{b}'_1 - \mathbf{b}_2 - \mathbf{b}'_2|)K_0(\sqrt{B_i}|\mathbf{b}_2 + \mathbf{b}'_2|)K_0(\sqrt{C_i}|\mathbf{b}_1|)K_0(\sqrt{D_i}|\mathbf{b}'_2|)$$

$$\Omega^{(k)} = (2\pi)^4 K_0(\sqrt{A_k}|\mathbf{b}_1 + \mathbf{b}'_1 - \mathbf{b}_2 - \mathbf{b}'_2|)K_0(\sqrt{B_k}|\mathbf{b}_2 + \mathbf{b}'_2|)K_0(\sqrt{C_k}|\mathbf{b}_1 - \mathbf{b}_2 - \mathbf{b}'_2|)K_0(\sqrt{D_k}|\mathbf{b}_2|)$$

$$\Omega^{(m)} = 8\pi^5 \int_0^1 dz_1 dz_2 \frac{1}{z_1(1-z_1)} \frac{\sqrt{X_2^m}}{\sqrt{|Z_2^m|}} K_1(\sqrt{X_2^m Z_2^m}) K_0(\sqrt{D_m}|\mathbf{b}_3|) \quad (44)$$

with

$$X_2^e = (\mathbf{b}'_2 + z_1\mathbf{b}_2)^2 + \frac{z_1(1-z_1)}{z_2}\mathbf{b}_2^2, Z_2^e = A_e(1-z_2) + \frac{z_2}{z_1(1-z_1)}[B_e(1-z_1) + C_e z_1]$$

$$Z_1^g = A_g z + B_g(1-z)$$

$$X_2^m = (\mathbf{b}'_2 + z_1\mathbf{b}_2)^2 + \frac{z_1(1-z_1)}{z_2}\mathbf{b}_2^2, Z_2^m = A_m(1-z_2) + \frac{z_2}{z_1(1-z_1)}[B_m(1-z_1) + C_m z_1] \quad (45)$$

Appendix E: Expressions for H_F^{ij}

In this appendix we list H_F^{ij} corresponding to the form factors defined in eq.(13). We use \tilde{F}_R^j for each diagram. The expressions for diagrams (a), (e), (g), (i), (k), and (m) in Fig. 1, whenever non-zero, are listed in the following. The expressions for diagrams (b), (f), (h), (j), (l) and (n) can be obtained by exchanging $x(x')_2$ and $x(x')_3$ and changing the signs for expressions $F_R^{V,T}$. Diagrams (c) and (d) have no contributions to $\Lambda_b \rightarrow \Lambda\gamma$. \tilde{F}_L is equal to zero in our approximation.

For the hard amplitudes of Fig.1(a):

$$\widetilde{F}_R^A = 8x_3\rho^2 M_{\Lambda_b}^4 \quad (46)$$

The relation between the tilde form factors listed above and the form factors in eq.(3) is as the following, taking \tilde{F}_R^A as an example, $F_R^A = \frac{\pi^2}{27} f_{\Lambda}^j f_{\Lambda_b} \int [Dx] \int [Db]^i C_l^{eff}(t^i) \Psi_{\Lambda_b}(x) \Phi_{\Lambda}^j(x') \exp[-S^i] \tilde{F}_R^A \Omega^i$. For this example $j = A$, and $f_{\Lambda}^A = f_{\Lambda}$. For Fig.1(a), 'i' takes the value 'a'. Similar for other form factors and diagrams.

The other non-zero contributions are

$$\begin{aligned} \text{Fig.1(e)} : \quad \widetilde{F}_R^V &= \widetilde{F}_R^A = -4M_{\Lambda_b}^4 \rho^2 x_3, \\ \text{Fig.1(g)} : \quad \widetilde{F}_R^V &= 4M_{\Lambda_b}^3 (m_b \rho + M_{\Lambda_b} (-2x_3(-1+\rho) + (1+x'_2(-1+\rho))\rho)) \\ \widetilde{F}_R^A &= 4M_{\Lambda_b}^3 (-1+\rho)(m_b + M_{\Lambda_b}(-1+x'_2\rho)), \\ \text{Fig.1(i)} : \quad \widetilde{F}_R^A &= 8M_{\Lambda_b}^3 x_2 (m_b(-1+\rho) + M_{\Lambda_b}(1+(-1+x'_1)\rho)), \\ \text{Fig.1(k)} : \quad \widetilde{F}_R^A &= 8M_{\Lambda_b}^3 \rho x'_2 (m_b + M_{\Lambda_b}(-1+\rho)), \\ \text{Fig.1(m)} : \quad \widetilde{F}_R^V &= -4M_{\Lambda_b}^2 (-m_b^2(-2+\rho) + M_{\Lambda_b} m_b (x_2 - x_2\rho + (-1+x'_1+x'_3)\rho) \\ &\quad + M_{\Lambda_b}^2 (-2 + (2-x'_1+x'_3)\rho - x'_3\rho^2 + x_2(1+(-1+x'_1)\rho))) \\ \widetilde{F}_R^A &= -4M_{\Lambda_b}^2 (m_b^2\rho + M_{\Lambda_b} m_b (-2+x_2(1+\rho) + (-1+x'_1+x'_3)\rho) \\ &\quad + M_{\Lambda_b}^2 (2 - (2+x'_1+x'_3)\rho + x'_3\rho^2 + x_2(-1+(1+x'_1)\rho))) \end{aligned} \quad (47)$$

-
- [1] CLEO Collaboration, M.S. Alam et al., Phys. Rev. Lett. **74** (1995) 2885.
 - [2] Belle Collaboration, P. Koppenburg et al., Phys.Rev.Lett. **93** (2004) 061803, BABAR Collaboration, B. Aubert et al., arXiv:hep-ex/0507001.
 - [3] Belle Collaboration, M. Nakao et al., Phys. Rev. **D69** (2004) 112001 ; BABAR Collaboration, B. Aubert et al., Phys. Rev. **D70** (2004) 112006.
 - [4] S. Bertonili, F. Borumati and A. Masiero, Phys. Rev. Lett. **59**, (1987) 180; Mikolaj Misiak, Nucl.Phys. **B393** (1993) 23; K. Adel, York-Peng Yao, Phys.Rev **D49**(1994) 4945; Christoph Greub, Tobias Hurth, Daniel Wyler Phys.Rev **D54** (1996) 3350; Nicolas Pott, Phys.Rev **D54** (1996) 938; X.-G. He, C.-S. Li and L.-L. Yang, Phys. Rev. **D71** (2005) 054006; Riccardo Barbieri, G.F. Giudice, Phys.Lett. **B309** (1993) 86; J. Hewett, Phys. Rev. Lett. **70** (1993) 1045; V. Barger, Berger and R. Phillips, Phys. Rev. Lett. **70** (1993) 1368.
 - [5] N. Deshpande et al., Phys. Rev. Lett. **59** (1987) 183; N.G. Deshpande, Josip Trampetic and Kuriakose Panose, Phys.Lett.**B214** (1988) 467; H.-N. Li and G.-L. Lin, Phys. Rev. **D60**, (1999) 054001; M. Beneke, T. Feldmann and D. Seidel, Nucl. Phys. **B612** (2001) 25; S. W. Bosch and G. Buchalla, Nucl. Phys. **B621** (2002) 459; Ahmed Ali and A.Y. Parkhomenko Eur.Phys.J **C23** (2002) 89.
 - [6] M. Beneke, G. Buchalla, M. Neubert and C.T. Sachrajda, Phys. Rev. Lett. **83** (1999) 1914; Nucl. Phys. **B591** (2000) 313; Nucl. Phys. **B606** (2001) 245.
 - [7] Yong-Yeon Keum and Hsiang-nan Li, Phys. Rev. **D63** (2001) 074006; Chuan-Hung Chen, Yong-Yeon Keum and Hsiang-nan Li, Phys. Rev. **D64** (2001) 112002; Yong-Yeon Keum, Hsiang-nan Li and A.I. Sanda, Phys. Rev. **D63** (2001) 054008; Chuan-Hung Chen, Yong-Yeon Keum and Hsiang-nan Li, Phys. Rev. **D66** (2002) 054013; Cai-Dian Lü, Kazumasa Ukai and Mao-Zhi Yang, Phys. Rev. **D63** (2001) 074009; Cai-Dian Lü and Mao-Zhi Yang, Eur. Phys. J. **C23** (2002) 275.
 - [8] C.-K. Chua, X.-G. He and W.-S. Hou, Phys. Rev. **D60**, (1999) 014003.
 - [9] T. Mannel and S. Recksiegel, J. Phys. **G24** (1998) 979.
 - [10] Chao-Shang Huang and Hua-Gang Yan, Phys. Rev. **D59** (1999) 114022.
 - [11] R. Mohanta, A.K. Giri, M.P. Khanna, M. Ishida and S. Ishida, Prog. Theor. Phys. **102** (1999) 645.
 - [12] H.Y. Cheng, C-Y. Cheung, G-L. Lin, Y.C. Lin, T.-M. Yan and H-L. Yu, Phys. Rev. **D51** (1995) 1199.
 - [13] Hsien-Hung Shih, Shih-Chang Lee and Hsiang-nan Li, Phys. Rev. **D59** (1999) 094014.

- [14] Hsien-Hung Shih, Shih-Chang Lee and Hsiang-nan Li, Phys. Rev. **D61** (2000) 114002.
- [15] Chung-Hsien Chou, Hsien-Hung Shih, Shih-Chang Lee and Hsiang-nan Li, Phys. Rev. **D65** (2002) 074030.
- [16] G. Buchalla, A.J. Buras and M.E. Lautenbacher, Rev. Mod. Phys. **68** (1996) 1125.
- [17] N.G. Deshpande, X.-G. He, J. Trampetic, Phys. Lett. **B367** (1996) 362.
- [18] W. Loinaz and R. Akhoury, Phys. Rev. **D53** (1996) 1416; F. Schlumpf, Ph.D. Thesis, Zurich University, 1992, arXiv:hep-ph/9211255.
- [19] V.L. Chernyak, A.A. Ogloblin and I.R. Zhitnitsky, Z. Phys. **C42** (1989) 569.
- [20] S. Eidelman, et al., Particle Data Group, Phys. Lett. **B592** (2004) 1.